Title
Characterization of the Corneal Subbasal Nerve Plexus in Limbal Stem Cell Deficiency

Journal
Cornea, 36(3)

ISSN
0277-3740

Authors
Chuephanich, Pichaya
Supiyaphun, Chantaka
Aravena, Carolina
et al.

Publication Date
2017-03-01

DOI
10.1097/ico.0000000000001092

Peer reviewed

HHS Public Access

Author manuscript

Cornea. Author manuscript; available in PMC 2018 March 01.

Published in final edited form as:

Cornea. 2017 March ; 36(3): 347–352. doi:10.1097/ICO.0000000000001092.

Characterization of Corneal Subbasal Nerve Plexus in Limbal Stem Cell Deficiency

Pichaya Chuephanich, MD[1,2], **Chantaka Supiyaphun, MD**[1,3], **Carolina Aravena, MD**[1,4], **Tahir Kansu Bozkurt, MD**[1], **Fei Yu, PhD**[1,5], and **Sophie X Deng, MD, PhD**[1,*]

[1]Cornea Division, Stein Eye Institute, University of California, Los Angeles [2]Department of Ophthalmology, Ramathibodi Hospital, Mahidol University, Bangkok, Thailand [3]Department of Ophthalmology, Vajira Hospital, Navamindradhiraj University, Bangkok, Thailand [4]Departamento de Oftalmología, Escuela de Medicina, Pontificia Universidad Católica de Chile, Santiago, Chile [5]Department of Biostatistics, Fielding School of Public Health, University of California, Los Angeles

Abstract

Purpose—To quantify the changes of subbasal nerve plexus in patients with limbal stem cell deficiency (LSCD) using in vivo laser scanning confocal microscopy. Design: Retrospective cross-sectional comparative study

Methods—Confocal images of 51 eyes of 37 patients with LSCD collected between 2010 and 2015 by the Heidelberg Retina Tomograph III Rostock Corneal Module Confocal Microscope. Two independent observers evaluated the scans of the central cornea. Seventeen normal eyes of 13 patients served as controls. Total subbasal nerve density (SND), density of long nerves (i.e., nerves 200 μm or longer) and the degree of tortuosity were quantified.

Results—The mean (± SD) total SND and long nerve density were 48.0 ± 34.2 nerves/mm^2 and 9.7 ± 10.9 nerves/mm^2, respectively, in all eyes with LSCD and 97.3 ± 29.9 nerves/mm^2 and 35.3 ± 25.3 nerves/mm^2, respectively, in eyes of the control group ($P<0.001$ for both comparisons). Compared with SND in control subjects, SND was reduced by 34.9% in the early stage, 54.0% in the intermediate stage, and 73.5% in the late stage of LSCD. The degrees of nerve tortuosity were significantly greater in patients with LSCD than in control subjects and differed among the early, intermediate, and late stages of LSCD. Reductions in total SND and long nerve density were positively correlated with the severity of LSCD.

Conclusions—Reductions in total SND and long nerve density were accompanied by increases in nerve tortuosity in eyes with LSCD. These parameters could be used as quantifiable measures of LSCD severity.

*Corresponding author: Sophie X. Deng, M.D., Ph.D., Cornea Division, Stein Eye Institute, University of California, Los Angeles, 100 Stein Plaza Los Angeles, CA 90095, Tel: 310-206-7202, Fax: 310-794-7906, deng@jsei.ucla.edu.

CONFLICT OF INTEREST: no conflicts of interest to disclose

FUNDING DISCLOSURES: This work was supported in part by an unrestricted grant from Research to Prevent Blindness. S.X.D received grant support from the National Eye Institute grants (5P30EY000331 and 1R01EY021797) and California Institute for Regenerative Medicine (TR2-01768, BF1-01768, CLIN1-08686).

Keywords

limbal stem cell deficiency; in vivo confocal microscopy; limbal stem cell; diagnosis; corneal nerve

Introduction

Limbal stem cells (LSCs) are stem cells located in the basal epithelial layer of the corneal limbus.[1] A sufficient number of functioning LSCs is required to maintain transparency of the cornea. The limbus is thought to function as a barrier between the cornea and conjunctival epithelial cells and prevent the conjunctival epithelium from migrating onto the corneal surface. Damage to the limbal areas by insults such as multiple surgeries, contact lens use, chemical injuries, drug toxicity, and chronic inflammation can lead to various degrees of limbal stem cell deficiency (LSCD).[2]

The diagnosis of LSCD is mainly based on history and clinical findings including opacity and irregularity of the corneal epithelium, recurrent epithelial defects, late fluorescein staining in a vortex pattern, neovascularization of the cornea, and the presence of goblet cells on the cornea confirmed by impression cytology.[3–5]

The diagnosis especially that of partial LSCD, remains challenging. The clinical presentations are subtle and non-specific, thus leading to misdiagnosis and delayed treatment. Impression cytology remains the diagnostic method for LSCD because this method can detect goblet cells on the cornea, which is an indication of the invasion of conjunctival epithelium onto the corneal surface.[3] However, goblet cell deficiency in conditions such as chemical or thermal injuries, Stevens-Johnson syndrome, or toxicity due to long-term topical use of glaucoma medications can be concurrent with LSCD and may lead to a false negative result.[6–8] There is no correlation of goblet cell density with the degree of LSCD. In addition, in the early or mild stage of LSCD, goblet cells may not be present on the cornea. Therefore, impression cytology has low sensitivity to make the diagnosis of LSCD. Currently, no standard classification system for LSCD has been established because of a lack of specific markers and quantitative methods to measure functional LSCs.

In vivo laser scanning confocal microscopy (IVCM) is a non-invasive diagnostic tool for obtaining high-resolution images with depth selectivity. Its ability to acquire images from selected depths enables the measurement of microstructural changes in various conditions[9–15]. Significant microstructure changes have been reported in patients with LSCD and include a decrease in basal epithelial cell density (BCD), epithelial thickness and subbasal nerve density (SND), and stage-dependent morphologic changes.[11, 16, 17] Although previous studies report a reduction in SND or even absence of subbasal nerve plexus in severe LSCD,[11, 18] the study populations were small and detail characterization of the nerve morphology was not performed. The purposes of the present study are to further characterize the morphological changes of subbasal nerve plexus, quantify the changes of subbasal nerve in different stages of LSCD and investigate whether the SND decrease is correlated with the severity of LSCD in a larger study population.

Materials and methods

The Institutional Review Board (IRB) at the University of California, Los Angeles, approved this retrospective cross-sectional comparative study prior to its initiation. Data collection was performed in a manner compliant with the Health Insurance Portability and Accountability Act (HIPPA), and the research adhered to the Declaration of Helsinki. All subjects were patients at the Stein Eye Institute, University of California, Los Angeles. Comprehensive examination using slit lamp biomicroscopy and IVCM was performed. Slit lamp photographs were taken. The diagnosis of LSCD was based on clinical evaluation by slit lamp examination and fluorescein-staining pattern according to the criteria previously reported.[11] Impression cytology was performed in 26 patients who were willing to undergo the test to confirm the diagnosis of LSCD. The three categories of disease severity were the early stage, characterized by the stippling or late fluorescein staining and a dull reflex; the intermediate stage, characterized by persistent late fluorescein staining in a vortex pattern that is associated with depression of the epithelial surface; and the late stage, characterized by vortex epithelial opacity as seen in the intermediate group with a history of a recurrent epithelial defect with or without vascularization of the cornea. The control group consisted of normal subjects without ocular pathology as indicated by slit lamp examination and without a previous history of ocular disease or ocular surface surgeries.

Confocal Microscopy Imaging

IVCM was performed by using the Heidelberg Retina Tomograph III Rostock Cornea Module (Heidelberg Engineering GmBH, Dossenheim, Germany). All eyes were anesthetized with proparacaine, 0.5% (Alcon Laboratories). Hydroxypropyl methylcellulose (Novartis Ophthalmics, Inc) was applied before the examination. A minimum of three scans of the central cornea focused on the nerves at the subbasal epithelial layer of each eye were collected.

Image Analysis

Two frames of the subbasal epithelium layer of the cornea each eye were selected to identify the subbasal nerve plexus characteristics, which were manually counted by two independent observers (P.C. and C.S.). Each image frame represented an area of 400 × 400 μm. The following criterion was used to select the frame for analysis: nerve segments were included in the counting if the area along the length of the nerves and their branches were visible. Dendritic cells and dendritic-like features were excluded from nerve analysis. The total number of the nerves in an image was counted and then the long nerves, which were defined as the nerves that were at least 200 μm long, were analyzed. This value, divided by the frame area (i.e., 0.16 $mm^{2)}$, yielded the total subbasal nerve density (SND) and long nerve density, respectively in nerves/mm^2. Morphology of the subbasal nerve plexus was defined as tortuosity and scored as grade 0, 1, or 2 according to the standard images shown in Figure 1. The currently published method or the automated system to grade tortuosity were not applicable to this study because the severity of the nerve dropout and tortuosity. We therefore established the grading scale as follows: grade 0 (F) was defined as straight, normal branching nerves with minimal tortuosity; grade 1 (G) was defined as moderate tortuosity with frequent changes of small amplitude in the direction of the nerve; and grade 2

(H) was defined as significant tortuosity with frequent changes of severe, abrupt amplitude in the nerve fiber direction.

Statistical Analysis

Statistical analyses were performed with SAS software version 9.4 (SAS, Inc, Cary, North Carolina, USA). Intra-class correlation coefficients were applied to assess the reliability of SND and long nerve density measurements obtained by two independent masked observers. Kruskal-Wallis test was used for the comparison of total SND and long nerve density among three subgroups (early, intermediate, and late stage) and the control group. Agreements of tortuosity between two graders were obtained. Any p values less than 0.05 were considered to indicate statistical significance.

Results

Fifty-one eyes of 37 patients diagnosed with LSCD and 17 eyes of 13 normal subjects from 2009 to 2015 were included in this study. The mean age was 55.0 years (range, 24–94 years) for the LSCD group and 52.0 years (range, 27–88 years) for the control group. Twenty-five eyes in the LSCD group were those of female patients and 26 were those of male patients. There was no statistically significant difference in age and gender between the control and LSCD groups (*t* test, $P = 0.25$ for both comparisons).

LSCD group was classified as early stage in 15 eyes (29.4%), intermediate stage in 30 eyes (58.8%), and late stage in 6 eyes (11.8%). Representative slit lamp photos showing fluorescein staining patterns of normal control and eyes at 3 stages of limbal stem cell deficiency are shown in Figure 2. The leading etiologies of LSCD were contact lens wear (15 eyes, 29.4%), followed by multiple surgeries (14 eyes, 27.5%), chronic inflammation (8 eyes, 15.7%), and drug toxicity (5 eyes, 9.8%). Patient demographic features, etiology of LSCD, clinical presentations, and stages of LSCD are listed in Supplemental Table 1. Presence of goblet cells on the cornea was detected in 13 eyes with LSCD.

As shown in Figure 1, there are striking changes in the morphology and density of the subbasal nerve plexus. In normal controls, the subbasal nerves are straight and the branches are often tangential (Figure 1, E). The number of subbasal nerve is greatly reduced in LSCD even at the early stage (Figure 1, F). The tortuosity might not be affected (Grade 0) or moderately affected (Grade 1). In eyes with intermediate or severe LSCD, the subbasal nerves are very torturous and have severe segmental enlargement or beading of the nerve (Figure 1, H). These dendritic-like nerve fibers are increasing common in more severe stage of LSCD. Some dendritic-like structures that does not appear to connect to any nerve fibers are also present and there is a complete absence of the normal straight nerve fibers. Whether these are fragments of nerve fibers or Langerhans cells is unclear.

To quantify the changes of subbasal nerve in LSCD, two independent observers performed the manual nerve counts and grading of the tortuosity in a masked fashion. There was high agreement between the two observers: the intra-class correlation coefficient (ICC) for the variability of total nerve density between two graders of 0.81. Bland-Altman plots of total

nerve and long nerve counts as determined by the two graders showing that there was no systematic bias in the grading between two graders (Supplemental Figure).

In all eyes with LSCD, the mean total SND ± SD and mean long nerve density ± SD were 48.0 ± 34.2 nerves/mm^2 and 9.7 ± 10.9 nerves/mm^2, respectively, which were significantly less than those in the control group (mean total SND ± SD, 97.3 ± 29.9 nerves/mm^2; mean long nerve density ± SD, 35.3 ± 25.3 nerves/mm^2; P<0.0001 for each comparison, Supplemental Table 2).

Analysis within the subgroups of patients with LSCD showed that the mean total SND and mean long nerve density were 63.3 ± 20.0 nerves/mm^2 and 18.1 ± 11.8 nerves/mm^2, respectively, in the early stage; 44.8 ± 38.1 and 6.6 ± 8.8 nerves/mm^2, respectively, in the intermediate stage; and 25.8 ± 28.6 and 3.9 ± 5.6 nerves/mm^2, respectively, in the late stage (Figure 2). When each subgroup of LSCD severity was compared with the control group, the percentages of SND reduction were 34.9% (P = 0.004) in the early stage, 54.0% (P <0.0001) in the intermediate stage, and 73.5% (P < 0.0001) in the late stage of LSCD. In addition, the percentages of long nerve density were significantly reduced in patients with LSCD than in the normal subjects (P < 0.0001, Figure 3). The reduction was 48.7% in the early stage, 81.3% in the intermediate stage, and 89.0% in the late stage. The differences in total SND and long nerve density among the three LSCD subgroups and the normal subjects were statistically significant for all comparisons (P < 0.0001).

Tortuosity of the subbasal nerve plexus was graded. In the control group, tortuosity in 14 eyes (82.4%) was grade 0, and tortuosity in 3 eyes (17.7%) was grade 1, which were significantly different (P < 0.0001) from the proportions of grades 0 and 1 in the LSCD group (Figure 4). The mean nerve tortuosity grade was 1.1 ± 0.5 in the early stage, 1.4 ± 0.5 in the intermediate stage, and 1.7 ± 0.6 in the late stage. All were significantly more than the mean nerve tortuosity grades in the control group (all P<0.05). Subbasal nerve plexus was not detected in 7 of 30 eyes (23.3%) in the intermediate stage of LSCD, 3 of 6 eyes (50.0%) in the late stage of LSCD, and none in the control group (Supplemental Table 2).

The leading etiology of LSCD in our series was contact lens wear. To exclude the possibility that the decrease in SND was due to the effect of contact lens wear alone and not a general phenomenon in LSCD, we performed comparisons of total SND and long nerve density between LSCD subjects who were contact lens wearers (15 eyes, 29.4%) and those who were not (36 eyes, 70.6%). There were no significant differences between the two groups in terms of total SND (58.2 ± 33.1 nerves/mm^2 and 42.8 ± 34.2 nerves/mm^2, respectively; P = 0.1) and long nerve density (9.0 ± 9.4 nerves/mm^2 and 9.9 ± 11.5 nerves/mm^2, respectively; P = 0.9). The total SND and long nerve density reduction in non-contact lens wearers were also significantly less than the values of the control group (P < 0.0001). This result indicates that the reduction in total SND and long nerve density are a general phenomenon in LSCD and not unique to the effect of contact lens.

Discussion

IVCM is a non-invasive imaging modality that has been used to study the microstructure of the cornea and diagnose various diseases.[4, 9–11, 13–16] The advantages of IVCM allow us to examine corneal nerve morphology and density in great detail.[10] The normal subbasal nerve plexus structure in healthy subjects has been studied.[15, 19, 20] Different features have been used previously to identify functioning subbasal nerve plexus.[19–27] Different features have been used such as the number of nerves present in one image, nerve density, which is defined as the total length of the nerve fibers (in micrometers) present in one image; the number of beadings; the branching pattern; and the grade of nerve tortuosity. Because of these variations of methodology, at the present time, there is a lack of consensus to quantify and characterize SND in a normal, healthy central cornea. Another challenge of quantification of nerve fibers is a lack of a reliable automated nerve counting software.

The subbasal nerve plexus morphology in patients with LSCD has distinct changes (Figure 1) such as severe nerve dropout, short nerve branch and sharp turn of the branched nerve. Some of the truncated nerve fragments had segmentally increased nerve diameter and had very short length. As a result of these changes, the subbasal nerve plexus could be mischaracterized as dendritic cells. The SND could be overestimated by their morphologic change to short and truncated individual nerves instead of a continuous single nerve fiber. Because of the drastic changes in the nerve morphology and nerve dropout, the subbasal nerves were counted manually to confirm the morphology of the nerve and the density of long nerve was added as another parameter to quantify the changes.

Results of our previous study suggest that the total SND decreased in patients with LSCD.[11] The current study confirms this observation in a larger LSCD population. We further investigated long nerve density, and nerve tortuosity in relation to the degree of LSCD and compared the number of total SND and long nerve density and morphologic changes in LSCD patients with those in normal subjects. The degree of reduction was positively correlated with the degree of LSCD. A significant reduction in SND (34.7%) was already detected in the early stage of LSCD, and a further decrease was seen in intermediate and late stages.

A decrease in SND has been observed in different pathological entities. For instance, the mean nerve fiber density in a group with non-proliferative diabetic retinopathy was 24.3% lower than that in normal subjects; the reduction in patients with proliferative diabetic retinopathy was 39.9%.[28] An 88.1% reduction in subbasal nerve length accompanied by an increase of hyper-reflective keratocytes has been observed in patients with neurotrophic keratitis.[29] Compared with normal subjects, patients with herpes zoster ophthalmicus (HZO) had a mean reduction of 75.7% in total nerve length and of 58.8% in the total number of nerves.[23] The mean nerve density was 80.1% lower in patients with herpes simplex viral (HSV) keratitis than in the control group, and the total nerve number in this patient group was 60.3% lower than that in the control.[10] There were a decrease in the density and number of subbasal corneal nerves and an increase in tortuosity and nerve beadings in patients with dry eye syndrome and corneal neuropathy.[21, 25, 30, 31] These observations along with ours support the notion that a loss of connection between the healthy corneal epithelial cells and

corneal nerve fibers in LSCD may lead to a lack of nerve growth factors, which affects the maintenance of healthy nerves.[32]

Another observation is a complete nerve drop out in patients with LSCD: 23.3% of eyes with intermediate-stage LSCD and 50.0% with the late-stage LSCD. This complete nerve drop out has not been reported in other conditions such as HSV keratitis or HZO.[22,29] The subbasal nerves can directly influence or be influenced by the corneal epithelium.[19] Corneal nerve fibers support the maintenance of healthy corneal epithelial cells by secreting trophic factors such as neuropeptides and neurotransmitters that stimulate epithelial cell growth, proliferation, regeneration, differentiation, and possibly migration.[32–34] Corneal and limbal epithelial cells also secrete glial cell-derived nerve growth factors and nerve growth factors that have trophic effects on nerve fibers.[35] Therefore, it is not surprising to find that SND and long nerve density was significantly decreased in LSCD, a condition in which normal functional corneal epithelial cells are absent. The nerves could serve as a proxy for assessing the health or pathology of the corneal epithelial surface. An absence of nerves could be an important indicator of the severity of LSCD.

Morphologic changes as indicated by tortuosity grading were also investigated in patients with LSCD in the current study. At the present time, there is no standard consensus on the grading system of nerve tortuosity. Previous studies used manual and automated tracing to define the tortuosity mostly on the basis of the individual standard.[22, 24, 27, 30, 31, 36–38] We used a different grading scale (Figure 1) because of the different presentation and severe nerve drop out in LSCD. The degrees of tortuosity of the nerve differed significantly among the early, intermediate, and late stages of LSCD and increased in the more severe stages. The greater tortuosity appears to be an indication of higher metabolic activity, possibly directly related to the repair of the alterations observed at the epithelial level.[21] Therefore, a high tortuosity morphology of the subbasal nerve might reflect a more damaged corneal epithelium.

There are limitations to our study. Assessment of subbasal nerve plexus requires visualization of the nerve fibers. Poor clarity of the corneal confocal images because of changes in the corneal extracellular matrix can obscure the visualization of the nerves and lead to an underestimate of nerve measurements. Because of the presence of conjunctival cells and inflammatory cell infiltration during the late stage of LSCD, an increase in the reflectivity of the corneal stroma could be present. In such a setting, there may be under-detection of the subbasal nerve as well.

In conclusion, total SND and long nerve density are significantly decreased in LSCD, whereas nerve tortuosity is increased. A complete nerve drop out was present in the severe LSCD. These parameters could be used in combination with clinical presentation, basal epithelial cell density, and epithelial thickness to stage the degree of LSCD. Further long-term studies are needed to investigate whether these nerve changes are reversible after successful LSC therapy.

Supplementary Material

Refer to Web version on PubMed Central for supplementary material.

References

1. Pellegrini G, Golisano O, Paterna P, et al. Location and clonal analysis of stem cells and their differentiated progeny in the human ocular surface. J Cell Biol. 1999; 145:769–82. [PubMed: 10330405]
2. Sejpal K, Bakhtiari P, Deng SX. Presentation, diagnosis and management of limbal stem cell deficiency. Middle East Afr J Ophthalmol. 2013; 20:5–10. [PubMed: 23580847]
3. Puangsricharern V, Tseng SC. Cytologic evidence of corneal diseases with limbal stem cell deficiency. Ophthalmology. 1995; 102:1476–85. [PubMed: 9097795]
4. Barbaro V, Ferrari S, Fasolo A, et al. Evaluation of ocular surface disorders: a new diagnostic tool based on impression cytology and confocal laser scanning microscopy. Br J Ophthalmol. 2010; 94:926–32. [PubMed: 19740872]
5. Donisi PM, Rama P, Fasolo A, et al. Analysis of limbal stem cell deficiency by corneal impression cytology. Cornea. 2003; 22:533–8. [PubMed: 12883346]
6. Arici MK, Arici DS, Topalkara A, et al. Adverse effects of topical antiglaucoma drugs on the ocular surface. Clin Experiment Ophthalmol. 2000; 28:113–7. [PubMed: 10933774]
7. Fatima A, Iftekhar G, Sangwan VS, et al. Ocular surface changes in limbal stem cell deficiency caused by chemical injury: a histologic study of excised pannus from recipients of cultured corneal epithelium. Eye (Lond). 2008; 22:1161–7. [PubMed: 17558385]
8. Herreras JM, Pastor JC, Calonge M, et al. Ocular surface alteration after long-term treatment with an antiglaucomatous drug. Ophthalmology. 1992; 99:1082–8. [PubMed: 1495787]
9. Wang Y, Le Q, Zhao F, et al. Application of in vivo laser scanning confocal microscopy for evaluation of ocular surface diseases: lessons learned from pterygium, meibomian gland disease, and chemical burns. Cornea. 2011; 30(Suppl 1):S25–8. [PubMed: 21912225]
10. Cruzat A, Pavan-Langston D, Hamrah P. In vivo confocal microscopy of corneal nerves: analysis and clinical correlation. Semin Ophthalmol. 2010; 25:171–7. [PubMed: 21090996]
11. Deng SX, Sejpal KD, Tang Q, et al. Characterization of limbal stem cell deficiency by in vivo laser scanning confocal microscopy: a microstructural approach. Arch Ophthalmol. 2012; 130:440–5. [PubMed: 22159172]
12. Lum E, Golebiowski B, Swarbrick HA. Mapping the corneal sub-basal nerve plexus in orthokeratology lens wear using in vivo laser scanning confocal microscopy. Invest Ophthalmol Vis Sci. 2012; 53:1803–9. [PubMed: 22395884]
13. Nubile M, Lanzini M, Miri A, et al. In vivo confocal microscopy in diagnosis of limbal stem cell deficiency. Am J Ophthalmol. 2013; 155:220–32. [PubMed: 23127748]
14. Vera LS, Gueudry J, Delcampe A, et al. In vivo confocal microscopic evaluation of corneal changes in chronic Stevens-Johnson syndrome and toxic epidermal necrolysis. Cornea. 2009; 28:401–7. [PubMed: 19411958]
15. Zhivov A, Winter K, Hovakimyan M, et al. Imaging and quantification of subbasal nerve plexus in healthy volunteers and diabetic patients with or without retinopathy. PLoS One. 2013; 8:e52157. [PubMed: 23341892]
16. Chan EH, Chen L, Rao JY, et al. Limbal Basal Cell Density Decreases in Limbal Stem Cell Deficiency. Am J Ophthalmol. 2015; 160:678–84. e4. [PubMed: 26149968]
17. Chan EH, Chen L, Yu F, et al. Epithelial Thinning in Limbal Stem Cell Deficiency. Am J Ophthalmol. 2015; 160:669–77. e4. [PubMed: 26163009]
18. Araujo AL, Ricardo JR, Sakai VN, et al. Impression cytology and in vivo confocal microscopy in corneas with total limbal stem cell deficiency. Arq Bras Oftalmol. 2013; 76:305–8. [PubMed: 24232946]

19. Parissi M, Karanis G, Randjelovic S, et al. Standardized baseline human corneal subbasal nerve density for clinical investigations with laser-scanning in vivo confocal microscopy. Invest Ophthalmol Vis Sci. 2013; 54:7091–102. [PubMed: 24084094]
20. Patel DV, McGhee CN. Mapping of the normal human corneal sub-Basal nerve plexus by in vivo laser scanning confocal microscopy. Invest Ophthalmol Vis Sci. 2005; 46:4485–8. [PubMed: 16303938]
21. Benitez-Del-Castillo JM, Acosta MC, Wassfi MA, et al. Relation between corneal innervation with confocal microscopy and corneal sensitivity with noncontact esthesiometry in patients with dry eye. Invest Ophthalmol Vis Sci. 2007; 48:173–81. [PubMed: 17197530]
22. Dabbah MA, Graham J, Petropoulos I, et al. Dual-model automatic detection of nerve-fibres in corneal confocal microscopy images. Med Image Comput Comput Assist Interv. 2010; 13:300–7. [PubMed: 20879244]
23. Hamrah P, Cruzat A, Dastjerdi MH, et al. Unilateral herpes zoster ophthalmicus results in bilateral corneal nerve alteration: an in vivo confocal microscopy study. Ophthalmology. 2013; 120:40–7. [PubMed: 22999636]
24. Oliveira-Soto L, Efron N. Morphology of corneal nerves using confocal microscopy. Cornea. 2001; 20:374–84. [PubMed: 11333324]
25. Aggarwal S, Kheirkhah A, Cavalcanti BM, et al. Autologous Serum Tears for Treatment of Photoallodynia in Patients with Corneal Neuropathy: Efficacy and Evaluation with In Vivo Confocal Microscopy. Ocul Surf. 2015; 13:250–62. [PubMed: 26045233]
26. Patel DV, McGhee CN. In vivo confocal microscopy of human corneal nerves in health, in ocular and systemic disease, and following corneal surgery: a review. Br J Ophthalmol. 2009; 93:853–60. [PubMed: 19019923]
27. Scarpa F, Grisan E, Ruggeri A. Automatic recognition of corneal nerve structures in images from confocal microscopy. Invest Ophthalmol Vis Sci. 2008; 49:4801–7. [PubMed: 18614801]
28. Nitoda E, Kallinikos P, Pallikaris A, et al. Correlation of diabetic retinopathy and corneal neuropathy using confocal microscopy. Curr Eye Res. 2012; 37:898–906. [PubMed: 22632054]
29. Lambiase A, Sacchetti M, Mastropasqua A, et al. Corneal changes in neurosurgically induced neurotrophic keratitis. JAMA Ophthalmol. 2013; 131:1547–53. [PubMed: 24158681]
30. Rosenthal P, Borsook D. The corneal pain system. Part I: the missing piece of the dry eye puzzle. Ocul Surf. 2012; 10:2–14. [PubMed: 22330055]
31. Labbe A, Alalwani H, Van Went C, et al. The relationship between subbasal nerve morphology and corneal sensation in ocular surface disease. Invest Ophthalmol Vis Sci. 2012; 53:4926–31. [PubMed: 22695962]
32. You L, Kruse FE, Volcker HE. Neurotrophic factors in the human cornea. Invest Ophthalmol Vis Sci. 2000; 41:692–702. [PubMed: 10711683]
33. Garcia-Hirschfeld J, Lopez-Briones LG, Belmonte C. Neurotrophic influences on corneal epithelial cells. Exp Eye Res. 1994; 59:597–605. [PubMed: 9492761]
34. Qi H, Li DQ, Bian F, Chuang EY, et al. Expression of glial cell-derived neurotrophic factor and its receptor in the stem-cell-containing human limbal epithelium. Br J Ophthalmol. 2008; 92:1269–74. [PubMed: 18723744]
35. Qi H, Chuang EY, Yoon KC, et al. Patterned expression of neurotrophic factors and receptors in human limbal and corneal regions. Mol Vis. 2007; 13:1934–41. [PubMed: 17982417]
36. Scarpa F, Zheng X, Ohashi Y, et al. Automatic evaluation of corneal nerve tortuosity in images from in vivo confocal microscopy. Invest Ophthalmol Vis Sci. 2011; 52:6404–8. [PubMed: 21775658]
37. Kallinikos P, Berhanu M, O'Donnell C, et al. Corneal nerve tortuosity in diabetic patients with neuropathy. Invest Ophthalmol Vis Sci. 2004; 45:418–22. [PubMed: 14744880]
38. Lagali N, Poletti E, Patel DV, et al. Focused tortuosity definitions based on expert clinical assessment of corneal subbasal nerves. Invest Ophthalmol Vis Sci. 2015; 56:5102–9. [PubMed: 26241397]

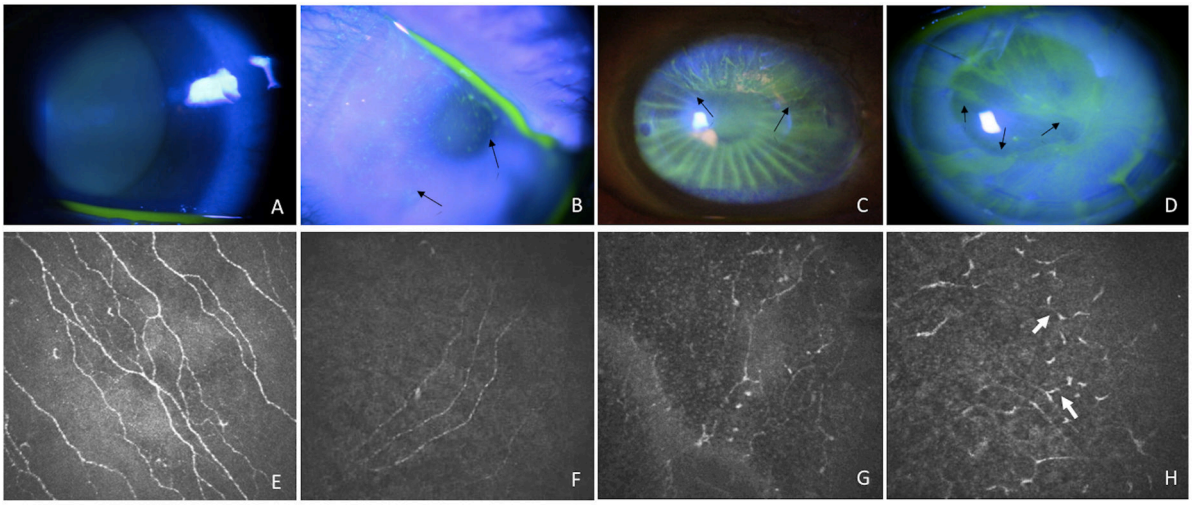

Figure 1.

Representative slit lamp photos showing fluorescein staining patterns of normal control (A) and eyes at 3 stages of limbal stem cell deficiency. The early stage (B), characterized by the diffuse stippling fluorescein staining. The intermediate stage (C), characterized by fluorescein staining in a vortex pattern and epithelial thinning in the superior quadrant of the cornea (arrows) and late stage (D), characterized by diffuse vortex epithelial fluorescein staining and epithelial thinning. Only one clock hour of the corneal surface is not affected. The edge of involvement in all stages is outlined by arrows. Example confocal images depicting tortuosity grades of the subbasal nerve plexus (E–H). A picture of the subbasal nerve plexus of a healthy, non-contact lens wearing subject served as a control (E). Grade 0 (E, F) was defined as straight, normal branching nerves with minimal tortuosity. Even though the subbasal nerve density was reduced in limbal stem cell deficiency (F), the nerve fibers remained fairly straight. Grade 1 (G) was defined as moderate tortuosity and frequent changes of small to moderate amplitude in the direction of the nerve. Grade 2 (H) was defined as significant tortuosity with frequent changes of severe, abrupt amplitude in the nerve fiber direction. Severe segmental enlargement of the nerve fibers was often present (white arrows).

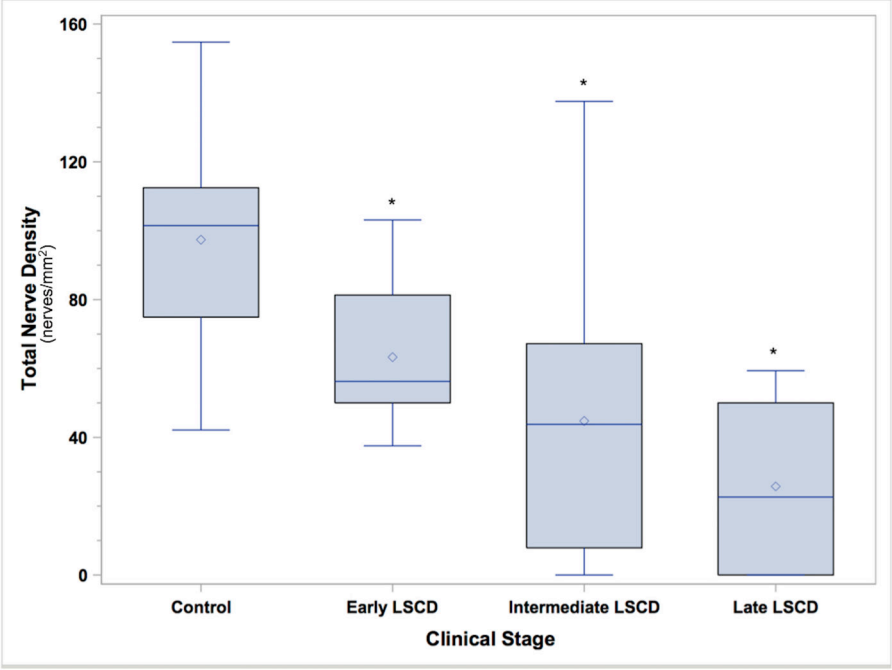

Figure 2.

Box and whisker plot of total nerve density (nerves/mm^2) in the control group (C) and in patients with LSCD in the early stage (E), intermediate stage (I), or late stage (L). The total SND in all patients with LSCD was significantly less than that in the controls. Asterisk denotes $P < 0.0001$.

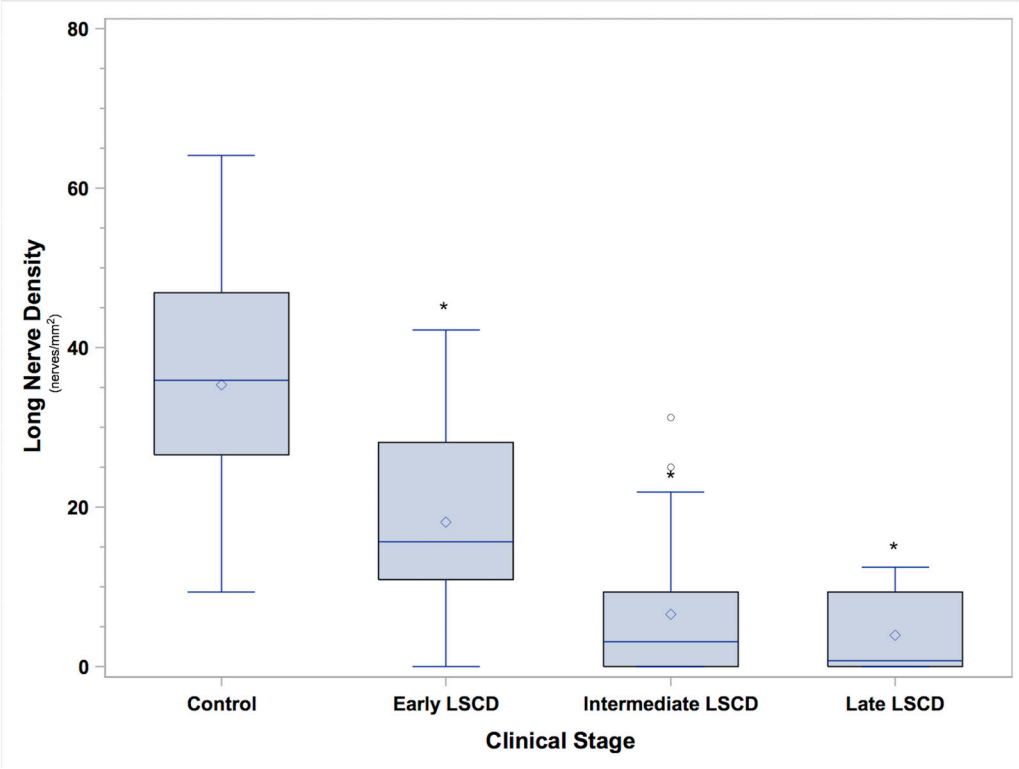

Figure 3.

Box and whisker plot of long nerve density (nerves/mm^2) in the control group (C) and in patients with LSCD in the early stage (E), intermediate stage (I), or and late stage (L). The long nerve density in all patients with LSCD was significantly less than that in the controls. Asterisk denotes $P < 0.0001$.

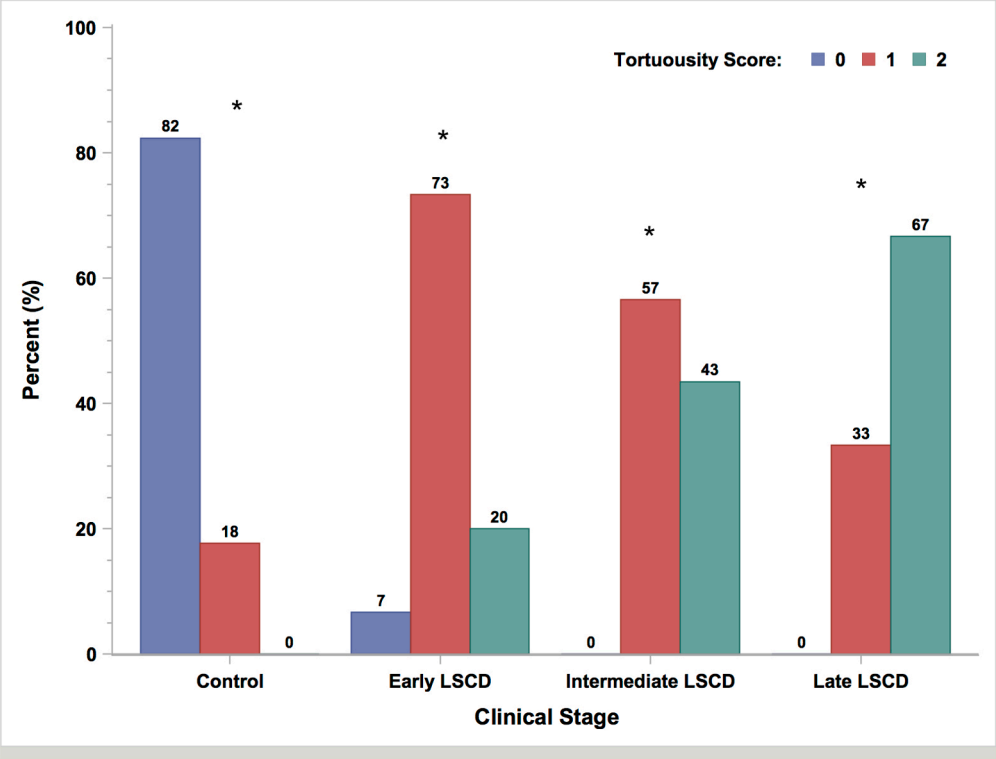

Figure 4.

Bar graph plot of nerve tortuosity in the control group and LSCD subgroups. The degrees of nerve tortuosity in all patients with LSCD significantly differed from those in controls. Asterisk denotes $P < 0.0001$.